



PROMOTION OF Pt-SUPPORTED NaY ZEOLITE WITH COPPER: ACTIVITY TOWARDS CO OXIDATION

ZEINHOM M. EL-BAHY^{a,b*}, AHMED I. HANAFY^{a,b} and SALAH M. EL-BAHY^c

^aChemistry Department, Faculty of Science, Taif University, TAIF, SAUDI ARABIA

^bChemistry Department, Faculty of Science, Al-Azhar University, Nasr City 11884, CAIRO, EGYPT

^cChemistry Department, Faculty of Medical and Applied Science, Taif University, TAIF, SAUDI ARABIA

ABSTRACT

Low temperature CO oxidation and adsorption over Cu-promoted and unpromoted PtY catalysts were investigated using *in situ* FTIR technique. The catalysts were prepared by ion exchange method of NaY in aqueous solutions of Pt²⁺ and/or Cu²⁺. The prepared catalysts were subjected to thermal treatment at 500°C prior to characterizations and gas adsorptions. The physicochemical characterization of the prepared solids was probed using X-ray diffraction (XRD), Fourier-transform infrared spectroscopy (FTIR), surface area measurements at -196°C, temperature programmed desorption (TPD) and *in situ* FTIR measurements of CO adsorption. The FTIR spectra and XRD patterns proved the preservation of zeolite structure after metals loading. Introduction of copper to Pt supported on Y zeolite decreased metal particle size from ≈ 20 to 14 nm as calculated from XRD patterns. The main product of CO+O₂ adsorption was CO₂, however, it was (-CO₃²⁻) in case of CO + H₂O adsorption (water gas shift reaction, WGS). Cu-promoted PtY had a pronounced catalytic activity towards CO oxidation more than Cu-free PtY catalyst. The reduced catalysts showed higher catalytic activity towards CO oxidation more than that of the unreduced catalysts. A trace of H₂O had a positive effect on CO oxidation in presence of O₂ gas and enhanced the formation of CO₂.

Key words: CO Adsorption, CO Oxidation, WGS, PtCuY, Ion exchange, Water effect.

INTRODUCTION

Public health all over the world is concerned with toxic air pollutants, which are released from automobiles, industries, and power-generation units. These pollutants strongly affect human health and the environment including air, water and soil. Due to the incomplete

* Author for correspondence; E-mail: zeinelbahy2020@yahoo.com; Ph.: +966504665647

combustion of fuels in both otto and diesel engines, the amount of pollutant gases, such as CO, NO and several hydrocarbons has increased considerably in recent years¹. Recently, the oxidation of carbon monoxide has been a topic of immense importance to many industrial applications². Catalytic converters are used to treat automotive exhausts and oxidize CO and hydrocarbons to CO₂ to comply with emission standards³.

Because of their activity for hydrogenation, dehydrogenation, complete and selective oxidation reactions, supported noble metal catalysts are most widely used among heterogeneous catalysts⁴. Platinum containing catalysts are the most active catalysts that are used in a fuel processor due to their ability to operate at high temperatures and their resistance to deactivation in presence of CO₂ or H₂O. Among various supports, Y type zeolite is considered as promising to increase the catalytic activity of Pt containing catalysts in CO oxidation at low temperatures⁵. Modifying Pt-Al₂O₃ system by iron oxide increased the tolerance towards hexamethyldisiloxane (HMDS)⁶. Promotion of Pt supported on mordenite with Fe caused the increase of activity and selectivity of CO oxidation in PROX reaction⁷. In our previous work, it was clearly observed that the addition of Fe to PtY causes an increase in the catalytic activity towards CO oxidation in presence of O₂ and/or H₂O⁸. The area under peak of the products (which reflects the relative catalytic activity) increased more than 100 times after promotion with Fe. The activity is likely to be controlled via the Pt-promoter interface. Hence, it is important that there must be a direct contact and interaction between Pt and promoter to increase its catalytic activity⁹. It is difficult to get such interaction using conventional preparation methods such as impregnation or co-precipitation, however, ion exchange method was successfully tested and homogeneously distributed ions all over the surface were obtained⁸.

CuO has been used in various studies due to its great importance in catalysis and high catalytic performance. It has been known for its high activity in methanol synthesis^{10,11}. Cu metal was used to modify precious metals such as Au supported on zeolites in the oxidation of CO¹²⁻¹⁵. Moreover, the addition of Cu to Pt greatly enhanced the activity of CO oxidation at low temperature over Nb₂O₃¹⁶ and it promoted the oxidation of CO by O₂ over Pt/Al₂O₃² or in PROX reaction¹⁷. On the other hand Cu decreased the conversion of CO over Al₂O₃ at low temperature^{16,18}.

The present study reports the preparation and characterization of simple metal-Y (PtY and CuY) and Cu-promoted PtY catalysts. An investigation using *in-situ* FTIR of CO adsorption and oxidation was carried out to emphasize the effect of Cu on PtY catalyst under ambient conditions. The effect of trace amount of water was studied as well.

EXPERIMENTAL

Catalyst preparation

Platinum and copper supported Y zeolite (PtY and CuY) powders were prepared according to the procedure described in a previous study⁸. Briefly, a sample (4 g) of NaY (Toyota Company Ltd., Japan) was mixed with 0.01 M solution of $\text{Pt}(\text{NH}_3)_4\text{Cl}_2 \cdot \text{H}_2\text{O}$ (Mtsuwa's Pure Chemicals) and $\text{Cu}(\text{CH}_3\text{COO})_2 \cdot \text{H}_2\text{O}$. The mixtures were stirred at room temperature (RT) for 24 hr. The suspensions were filtered off and the process was repeated three times until almost complete exchange was obtained.

The same method was used as well to prepare Cu-promoted PtY (PtCuY) by successive addition of aqueous solutions of Cu^{2+} and Pt^{2+} to NaY zeolite. Cu^{2+} (0.01 M) was introduced at first to the weighed amount of NaY (4 g) and continuously stirred for 1 hr at room temperature. The solution was centrifuged and washed with distilled water several times. The obtained paste was dried at 100°C for 24 hr and finally calcined at 500°C for 3 hr. CuY powder was added to Pt^{2+} aqueous solution [$\text{Pt}(\text{NH}_3)_4\text{Cl}_2 \cdot \text{H}_2\text{O}$, 0.01 M]. The solution containing CuY suspension was stirred at 80°C for 1 hr before filtering, washing with distilled water and finally drying at 100°C for 24 hr.

Reduction of the catalysts was performed using 80 torr of H_2 atmosphere in closed vacuum system for 30 min at 400°C in presence of liquid nitrogen trap. Reduced sample will be referred as PtY(R) and PtCuY(R) for free and Cu-promoted PtY catalysts, respectively.

The Pt content was measured by atomic absorption spectroscopy using Varian atomic absorption spectrometer (Shimadzu AA-6400F) and it was found to be ≈ 1.2 wt%.

Catalyst characterization

The synthesized catalysts were characterized using different spectroscopic techniques to collect some information about their structural properties. X-ray diffraction (XRD) was performed using Bruker axis, D8-Advance diffractometer employing Cu-K α radiation (wavelength 154.056 pm) with scanning rate of 2° in 2 θ /min. Average crystallite size was calculated using Scherrer equation with Gaussian line shape approximation ($D = 0.89\lambda/\beta\cos\theta$)¹⁹, where D is the crystallite size, λ is the wavelength (1.5404 Å), β is the full width at half the maximum intensity (FWHM) in radians, and θ is the Bragg's angle.

FTIR spectra of the prepared samples at room temperature was carried out using solid state mixture pellets of sample/KBr. JASCO FTIR-600 Plus FT-IR spectrometer was used to measure FTIR spectra with accumulation of 100 scans and resolution of 2 cm^{-1} .

Temperature Programmed Desorption (TPD) experiments were performed using CO gas as a probe molecule in a fixed-bed reactor cell. Prior to all measurements, a sample weight 30 mg of the catalyst powder was treated at 500°C for 1 hr in air. Then it was evacuated for another 1 h at the same temperature under vacuum (10^{-4} torr). The sample was then left to cool to RT after, which 7 torr of CO were admitted to the reactor cell and left for 30 min to equilibrate. The samples were degassed at RT for 1 hr and then the TPD profiles were recorded by linear heating of the samples during raising the temperature from RT to 700°C with ramp rate of 5°C/min. To test and compare the possibility of CO₂ desorption out of the surface, a mixture of CO + O₂ (7:7) was admitted to the cell containing the solid sample. The degassed species (CO, $m/z = 28$; CO₂, $m/z = 44$) were monitored by a gas desorption analyzer (ANELVA, M-QA100TS) equipped with a quadruple mass analyzer in a high-vacuum chamber of 7.5×10^{-9} torr.

The surface area measurements and the porous properties were obtained by N₂ adsorption–desorption isotherms at -196°C in a Quantachrome AS1Win. (Quantachrome instruments Version 2.01). Priors to adsorption and measurements, all samples were heated under vacuum at 300°C for 2 h. The surface area was calculated in the (P/P_0) range of 0.02–0.25 using Brunauer–Emmett–Teller (BET) method. The total pore volume was determined from the monolayer adsorption value at $P/P_0 \approx 0.95$. Pore size and pore volume were calculated from t -plot analysis of the isotherms data.

One of the most powerful characterization techniques is the IR spectroscopy of adsorbed probe molecules, which is used for the investigation of surface active sites. CO adsorption experiments were carried out using *in-situ* FTIR technique. JASCO FTIR-660 Plus was used to record the spectra with accumulation and spectral resolution of 32 scans and 2 cm⁻¹, respectively. A weight of 15-20 mg/cm² of the powder of each sample was pressed as self-supporting pellet which was treated directly in a special purpose-made IR quartz cell. The cell was equipped with CaCl₂ windows. The pellets in the cell were heated in air for 2 hr at 500°C followed by 1 h evacuation ($< 10^{-4}$ torr) at the same temperature. The cell was then left to cool to RT after which a dose of 10 torr of CO gas was admitted to the cell and it was left to equilibrate for 30 min. The sample was then evacuated for 20 min at RT before closing the cell with built in stopcock. The cell was removed from the vacuum line and placed in the IR instrument for spectral recording. The spectral changes due to CO admission was determined by subtraction of the background spectrum measured before gas admission.

The spectra changes after admission of gas mixtures will be traced by the same above technique as well. The samples were activated by heating at 500°C for 2 hr in air

followed by 1 hr evacuation at the same temperature. The gas mixtures were admitted to the cell containing catalyst pellets after cooling at RT. The above procedure mentioned in CO adsorption experiments will be followed to determine the spectral changes after gas mixture admission. According to previous literature^{20,21}, the ratio $O_2/CO = 1$ was chosen to be used in the present study. *In-situ* FTIR spectra were obtained using reaction gas mixture conditions of $CO : O_2 = 10 : 10$ (total = 20 mm Hg) for CO oxidation; $CO : H_2O = 15 : 1$ (total = 16 mm Hg) for water gas shift reaction; and $CO : O_2 : H_2O = 15 : 15 : 1$ (total = 31 mmHg) for CO oxidation in presence of H_2O . The reaction was carried out at different contact times and temperatures as will be stated later.

RESULTS AND DISCUSSION

Characterization of the prepared catalysts

X-ray diffraction

XRD analysis is used in this study to identify the changes in the chemical phases of the prepared samples and correlate it with their activity in carbon monoxide oxidation. The XRD patterns of PtY, CuY and Cu-promoted PtY catalysts besides parent NaY zeolite are shown in Fig. 1. The patterns confirm the persistence of the zeolite structure. Small lines due to Pt (111) and Pt (200) were observed at 2θ values of 40.4° and 47° , respectively. It is clear also that the intensity (I) of the zeolite lines (220), (331) and (311) are in the order of $I_{331} > I_{220} > I_{311}$. This order indicates that the Pt or Cu are randomly distributed within the lattice^{8,22}. All samples did not show any lines characteristic to metallic copper or any of copper oxides.

The relative crystallinity was determined by comparing the main peaks intensities of the metal supported zeolite with that of parent NaY (100%). As indicated from Fig. 1, the structure and the relative crystallinity of the prepared samples has not been affected by loading metal oxides as summarized in Table 1. Pt particle size was reported to increase after addition of secondary metal of different preparation methods such as incipient wetness^{23,9} or chemical vapor deposition²⁴. Scherrer's equation was used to calculate the size of Pt particles and it was found to be ≈ 20 nm in case of PtY catalysts, whereas it is smaller in PtCuY (≈ 14 nm). This indicates that Pt particles undergo more dispersion with the addition of Cu. Such decrease in Pt particle size in binary system is in consistence with other reports in case of the addition of (Co and Ni)^{25,26} and Fe⁸ to PtY catalyst. This indicates that nanosized Pt particles are easily prepared by the employed ion exchange method.

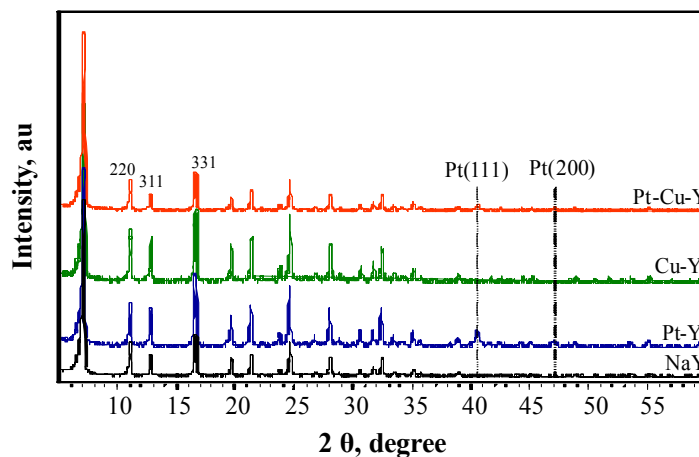


Fig. 1: X-ray powder diffraction patterns of parent NaY, PtY and Cu-promoted PtY catalysts

FTIR spectroscopy

The IR spectra of the prepared catalysts besides parent NaY zeolite were examined as shown in Fig. 2 to show the bonds in the zeolite framework. In the low wavenumber range of $1800\text{--}400\text{ cm}^{-1}$, the spectra exhibited bands at about 1184 , 1054 , 817 , 746 , 591 and 468 cm^{-1} with varying intensities and widths, which are characteristic of Y zeolite framework²⁷.

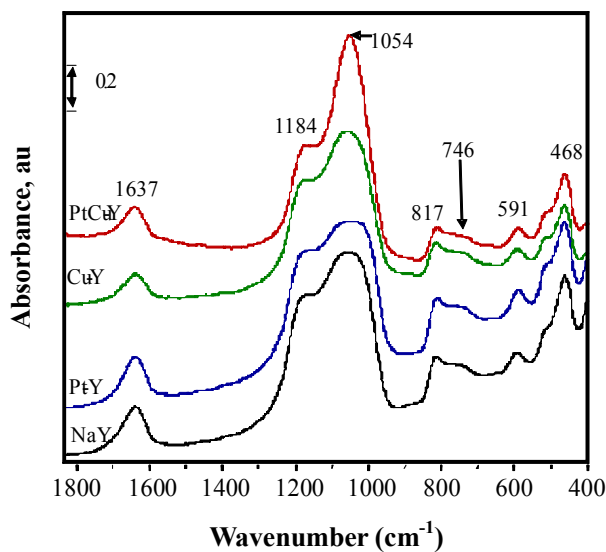


Fig. 2: FTIR spectra of parent NaY, PtY and Cu-promoted PtY catalysts

The bands at 1054, 746 and 468 cm^{-1} are due to the structural insensitive vibrations caused by internal vibrations of (Si,Al) O_4 tetrahedra of Y zeolite framework. Whereas the sensitive framework structure related to external linkages between (Si, Al) O_4 tetrahedra were observed at 1184, 817, and 591 cm^{-1} .²⁸ The absorption frequency of H_2O vapor was located at 1637 cm^{-1} .^{29,30} Because of its low concentration on the surface, Pt- or Cu-O bonds have not been detected in IR spectra. It is clear that the framework structure did not undergo significant changes after loading single or binary metal oxides on NaY zeolite as noticed before in XRD patterns.

Temperature programmed desorption (TPD)

The temperature programmed desorption profiles of the desorbed CO in the temperature range of 25–700°C for the prepared samples are shown in Fig. 3a. CO-TPD profile of PtY catalyst shows only one wide peak due to CO desorption at 364°C whereas the CO-TPD profile of CuY shows the CO desorption peak at 154°C and wide range desorption above 300°C. With respect to PtCuY desorption profile, one peak can be observed at 105°C. Also, small peak in the medium temperature range at 212°C and small wide peak above 400°C were observed for the same sample. It is clear from the desorption patterns that, PtCuY showed lower temperature desorption peak (105°C) compared to PtY and CuY samples. This indicates that PtCuY has lower molecular CO desorption energy due to the presence of low basicity sites. The CO-TPD patterns of CuY and PtCuY showed broad desorption peaks due to different activation energies for desorption. This indicates some heterogeneity in the adsorption sites on the surface^{31,32}. With careful inspection of Fig. 3a, it can be seen that the Pt peak disappeared after addition of Cu, which may be due to the coverage of Pt sites with Cu moieties. Also a shift to lower temperature of CO desorption from 154 to 105°C was noticed. This may be attributed to an interaction of Cu with Pt particles³³. These results indicated that the promotion of Pt with Cu caused the formation of Pt species with low basic sites that has different electronic characters and have weak interaction with CO molecules. The same observation was noticed previously in case of promoting Pt/ Al_2O_3 with Mg ions³⁴.

Fig. 3b shows the TPD profiles of CO_2 desorbed from PtY, CuY and PtCuY samples. A mixture of (CO + O_2 ; 7:7) was admitted to the solid sample. PtY catalyst exhibited a broad desorption peak at around 414°C with a shoulder above 490°C. These peaks are assigned to strong basic sites. In case of CuY, it presented very broad peak above 300°C. For PtCuY catalyst, two CO_2 desorption peaks around 212°C and 456°C were noticed. These peaks were assigned to weak and medium basic sites, respectively³⁴. These data points to the fact that the formation of CO_2 on PtCuY and its desorption out of the surface may occur at lower temperature than on the surface of either PtY or CuY.

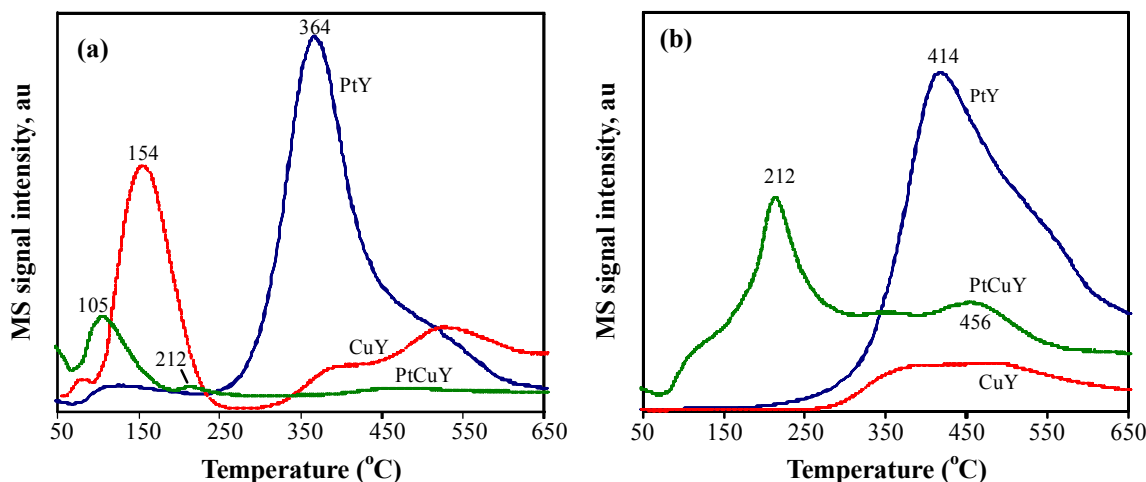


Fig. 3: TPD spectra of (a) CO desorption (b) CO₂ desorption profiles of PtY, CuY and PtCuY samples

Surface texture characteristics

The isotherms of N₂ adsorption of NaY, CuY, PtY and PtCuY were measured by N₂ adsorption at -196°C as shown in Fig. 4. The isotherms of all the samples, closely or faintly, resembled type IV according to the IUPAC classification which indicates the presence of both mesopores and micropores³⁵.

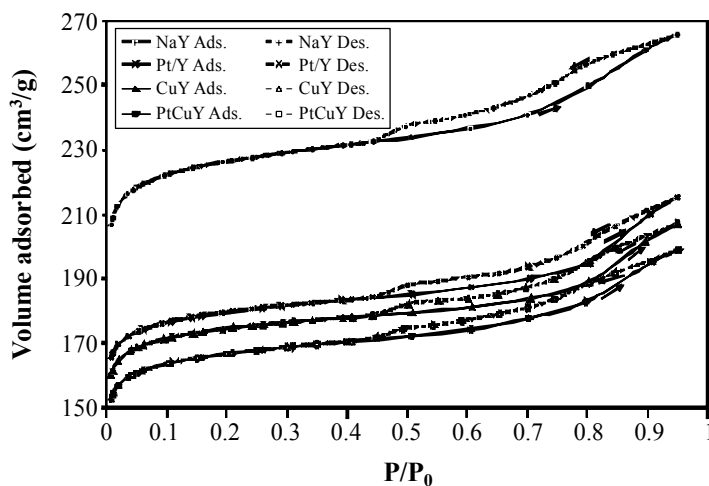


Fig. 4: Nitrogen adsorption-desorption isotherms for parent NaY and different metals loaded NaY catalysts

It is clear that, a relatively high adsorption was noticed below $P/P_0 < 0.1$ due to micropore filling. Increasing nitrogen pressure up to $P/P_0 = 0.7$ leads to a gradual increase in adsorption, which is followed by a sudden increase of adsorption until $P/P_0 = 0.95$. The overall adsorption was the highest in NaY (265 cm^3/g) while it was the lowest in PtCuY (195 cm^3/g). These values has direct impact on S_{BET} values as shown in Table 1. NaY presented both micropores and mesopores but these features slightly decreased after addition of metal ions. This is noticed by the small reduction of overall adsorption and the calculated pore volume and pore radius of these samples. Generally, most of the porosity character was maintained even after loading the single or binary systems, which is in consistence with XRD and FTIR data.

Table 1: Physical properties of the prepared catalysts

Sample	Crystallinity (%)	Surface area (m^2/g)	Overall adsorption (cm^3/g)	Pore size (cc/g)	Pore radius (\AA)	Particle size ^a (nm)
NaY	100	719	265	0.151	4.548	-
PtY	97	556	210	0.118	4.544	20
CuY	98	552	207	0.116	4.552	-
PtCuY	97	528	195	0.112	4.555	14a

^aParticle size calculated from XRD patterns

FTIR spectra of CO adsorption

In order to clarify the types of Cu and Pt species on Y zeolite, a comparative IR spectroscopic study of CO adsorption on the prepared samples was carried out. In these experiments, 10 torr of CO was added at room temperature to the as-prepared and reduced catalysts.

Adsorption of CO on PtY

Although CO adsorption on PtY at RT was discussed before in previous report of our group⁸, we will present and discuss it for the sake of comparison and the spectra are presented in Fig. 5. The admission of CO to PtY caused the appearance of small peaks due to $\text{Pt}^{n+}\text{-CO}$ ($2 \geq n \geq 0$) at 2168 (small), 2128 and 2076 cm^{-1} , Fig. 5a. The small peak at 2168 cm^{-1} is assigned to CO adsorbed on Pt ions in cationic positions³⁶. The peaks at 2128 and 2076 cm^{-1} are due to $\text{Pt}^+(\text{CO})_2$ and on-top linear $\text{Pt}^0\text{-CO}$ ³⁶⁻³⁸, respectively. Additionally, very small peak was detected at 1884 cm^{-1} due to bridged Pt_2^0CO ³⁹. With evacuation at RT,

Fig. 5b, an increase of the peaks at 2076 cm^{-1} ($\text{Pt}^0\text{-CO}$) increased, however, the peaks due to $\text{Pt}^{\text{n+}}\text{-CO}$ at 2168 and 2128 cm^{-1} decreased and the peak at 1884 cm^{-1} disappeared. A new small peak at 2355 cm^{-1} due to physically adsorbed CO_2 ⁴⁰ was also detected.

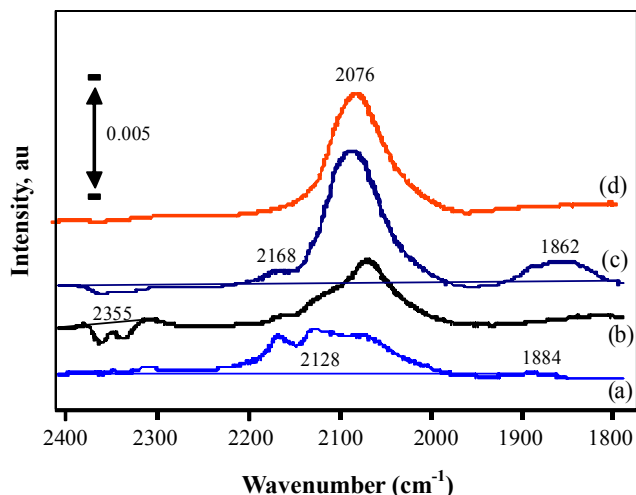


Fig. 5: FTIR spectra after admission of CO (10 torr) over PtY (a,b) and PtY(R) (c,d): a and c after 20 min of CO adsorption and (b and d) after evacuation at RT

On the other hand, the CO adsorption on reduced PtY(R) at RT, Fig. 5c, presented two relatively high intensity peaks at 2076 and 1862 cm^{-1} due to $\text{Pt}^0\text{-CO}$ and Pt_2CO , respectively. Platinum oxidized species still remained after reduction with H_2 . This was indicated by the presence of small intensity peak at 2168 cm^{-1} due to $\text{Pt}^{\text{n+}}\text{CO}$. After evacuation at RT, Fig. 5d, the peaks at 1862 and 2168 cm^{-1} disappeared, however, the peak characteristic of $\text{Pt}^0\text{-CO}$ was shifted to lower wavenumber without change in its intensity.

Adsorption of CO on CuY

It was reported in literature that no stable carbonyls can be formed when CO is adsorbed on Cu^{2+} sites at room temperature⁴¹⁻⁴³. Moreover, such species are stabilized by back π -donation on Cu^+ ions at the same temperature⁴⁴⁻⁴⁶. According to literature⁴⁷, CO bands above 2000 cm^{-1} are attributed to linearly bonded CO molecules. CO bands below 2100 cm^{-1} are due to $\text{Cu}^0\text{-CO}$. The vibrations above 2100 cm^{-1} are assigned to $\text{Cu}^{\text{n+}}\text{-CO}$. The addition of 10 torr CO as a reducing agent to the heat treated CuY, which includes Cu^{2+} , have led to the generation of a certain amount of Cu^+ ions as shown in Fig. 6. At RT, Fig. 6a, strong absorption band was observed at 2160 due to $\nu(\text{CO})$ stretching in CO adsorbed on dehydrated Cu^+Y ⁴⁸⁻⁵⁰. The second maximum peak was observed at 2140 cm^{-1} and was attributed to gas phase CO stretching frequency⁴⁸. A small peak at 2184 cm^{-1} was noticed

due to geminal $\text{Cu}^+(\text{CO})_2$ ^{42,51,52} and other tiny peak was detected at 2070 cm^{-1} , which is attributed to metallic $\text{Cu}^0\text{-CO}$ sites. With evacuation at RT and 50°C (Fig. 6b,c) the peak characteristic of gas phase CO at 2140 cm^{-1} decreased while all the other peaks were also still detected at 2184 , 2160 and 2070 cm^{-1} .

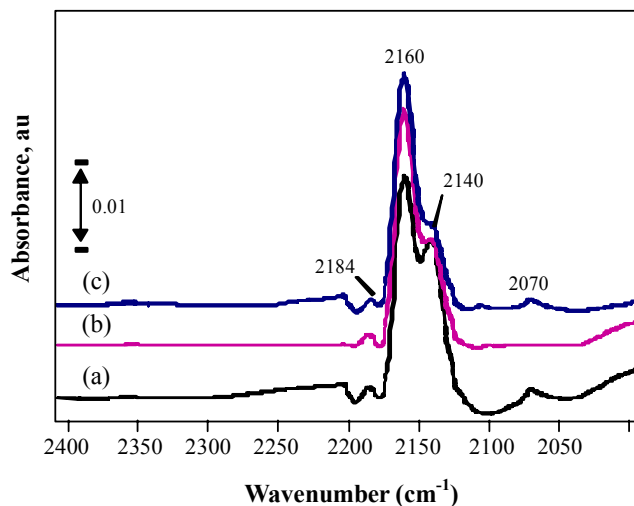


Fig. 6: FTIR spectra after admission of CO (10 torr) over CuY; (a) Gas phase adsorption, (b) evacuation at RT and (c) evacuation at 50°C

Adsorption of CO on PtCuY

Fig. 7 shows the infrared spectra of CO adsorbed on PtCuY and PtCuY(R) catalysts. The spectrum taken after CO adsorption over PtCuY at RT (Fig. 7a) displayed a well resolved strong absorption band at 2156 cm^{-1} corresponding to linear $\text{Cu}^+\text{-CO}$ with 4 cm^{-1} lower wavenumber than that of $\text{Cu}^+\text{-CO}$ in CuY sample (2160 cm^{-1}), which indicates the increase of back π -donation in presence of Pt. In addition, small peaks were detected at 2180 and 2124 cm^{-1} and were attributed to $\text{Cu}^+(\text{CO})_2$ and $\text{Pt}^+\text{-CO}$, respectively. After evacuation at RT (Fig. 7b) the intensity of all adsorption peaks decreased and vanished completely after evacuation at 50°C (Fig. 7c).

The spectrum recorded after admission of 10 torr of CO gas on the surface of PtCuY(R) at RT (Fig. 7d) showed the same peaks at 2181 and 2157 cm^{-1} , which are characteristic of $\text{Cu}^+(\text{CO})_2$ and $\text{Cu}^+\text{-CO}$, respectively. This indicates that the Cu^{2+} species changes to Cu^+ in the presence of either CO or H_2 . The spectrum showed also a peak at 2051 cm^{-1} due to linear $\text{M}^0\text{-CO}$ ($\text{M} = \text{Pt}$ and/or Cu). With evacuation at RT (Fig. 7e), the peak at 2181 cm^{-1} disappeared and the peak at 2157 cm^{-1} decreased with red shift = 6 cm^{-1}

(2145 cm^{-1}). With increasing evacuation temperature to 50°C (Fig. 7f), only the peak at 2045 cm^{-1} , which is due to $\text{M}^0\text{-CO}$ was detected. These adsorption data is in a good agreement with the TDP of CO adsorption which shows CO desorption peak due to Cu sites only. These results may lead to the conclusion that Cu^{n+} may be on the top of Pt particles, which is in agreement with the TDP data results.

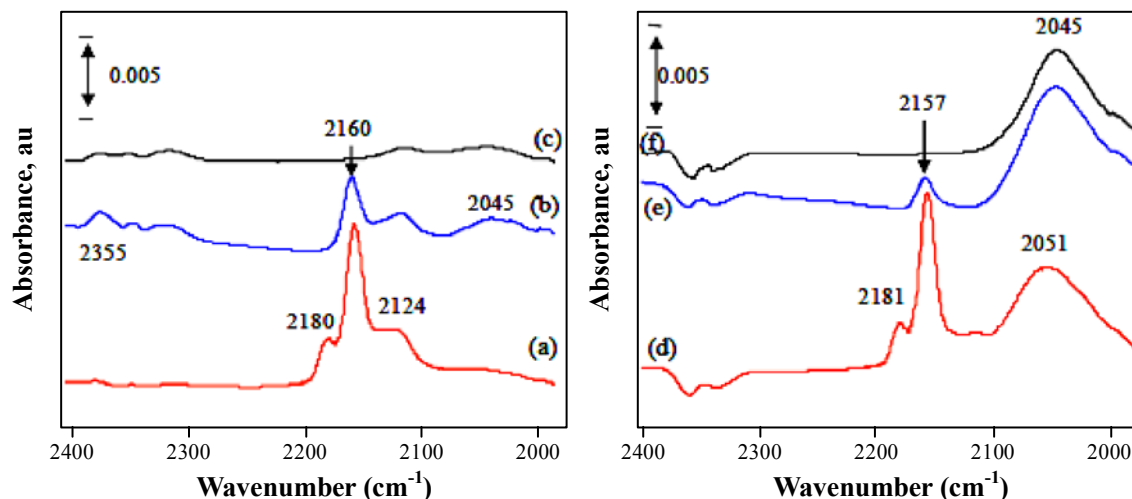


Fig. 7: FTIR spectra after admission of 10 Torr CO over PtCuY and PtCuY(R): (a and d) after 20 min of CO adsorption, (b and e) after evacuation at RT, (c and f) after evacuation at 50°C

The catalytic activity measurements of the prepared samples

CO oxidation over the prepared catalysts

CO oxidation over PtY

The IR spectra changes after addition of $\text{CO} + \text{O}_2$ ($\text{CO}/\text{O}_2 = 1$) to the cell containing platinum supported Y zeolite and the temperature dependence on these IR spectra were discussed in our previous work⁸ and are shown in Fig. 8. Only a small band at 2075 cm^{-1} , which was attributed to linear $\text{Pt}^0\text{-CO}$ was observed, Fig. 8a. Increasing the temperature of the cell to 50°C and 100°C, Fig. 8b,c leads to the appearance of two new peaks due to CO oxidation at 1710 and 2355 cm^{-1} which are due to carboxylate species and physisorbed CO_2 , respectively. In case of PtY(R) sample, the spectrum taken at RT is presented in Fig. 8d. It presents two peaks at 2090 and 1860 cm^{-1} due to linear $\text{Pt}^0\text{-CO}$ and bridged Pt^0_2CO , respectively. Only one oxidation product at RT was detected at 2355 cm^{-1} due to

physisorbed CO₂. Increasing the temperature to 50°C and 100°C leads to the increase of the peak at 2355 cm⁻¹ (physisorbed CO₂), however, unexpectedly, the peaks characteristic to on-top linear Pt⁰-CO (at 2090 cm⁻¹) and bridged Pt⁰₂CO (at 1860 cm⁻¹) increased. The increase of these peaks may indicate further transformation of Ptⁿ⁺ → Pt⁰ (reduction) under the present conditions²⁹. Carbonate or carboxylate species were not detected in this case i.e. CO₂ was the only oxidation product of CO on the surface of PtY(R). Carboxylate species were detected over the unreduced PtY catalyst, which contains less number of platinum sites. As discussed previously, the oxidation of CO over Pt sites follows Langmuir–Hinshelwood single site mechanism^{53,54}. It was explained in our previous report⁸ that carbonyl species (carboxylate and/or carbonate) may be considered as an intermediate to CO₂ on Pt sites on the surface of PtY catalyst.

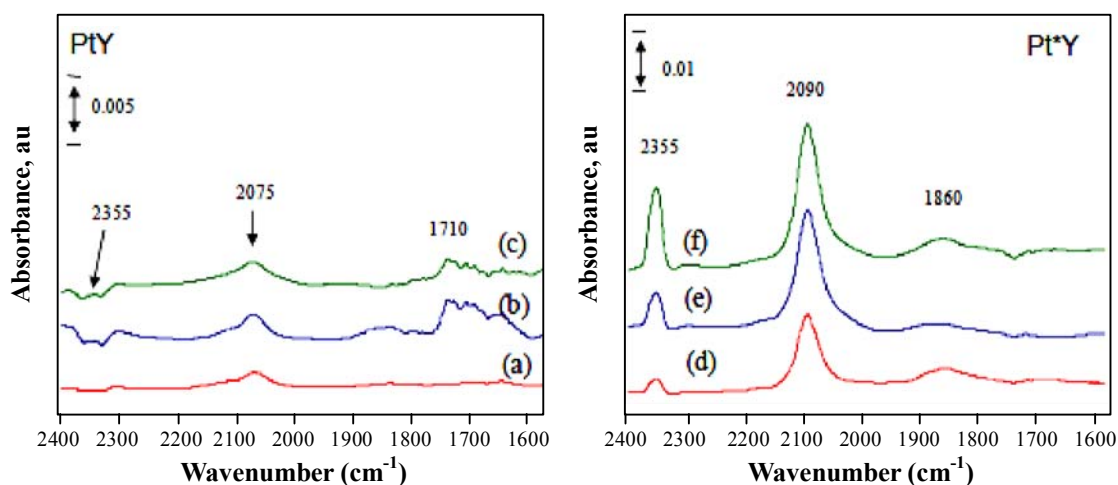


Fig. 8: *In situ* FTIR spectra of the CO + O₂ (10:10) gas mixture adsorbed on PtY and PtY(R) as a function of temperature; (a and d) RT, (b and e) heated at 50°C and (c and f) heated at 100°C

CO oxidation over CuY

Infra-red spectra after admission of the gas mixture CO + O₂ (CO/O₂ = 1) on the surface of CuY catalyst is presented in Fig. 9. In the range of 2400-1700 cm⁻¹, the spectra presented only the peaks characteristic to Cu⁺(CO)₂, Cu⁺-CO, and CO in gas phase at 2184, 2160 and 2140 cm⁻¹, respectively. However, the spectra did not show any CO oxidation product in the range of 2400-1700 cm⁻¹, which indicates that the Cuⁿ⁺ species has no catalytic activity towards CO oxidation at room temperature. This is in good agreement with other literature, which reported that the addition of Cu to Pt-Al₂O₃ decreased CO and O₂

conversions below 100°C and increased it above 100°C. This may be related to the low CO activation (chemisorptions and subsequent oxidation) below 100°C¹⁸.

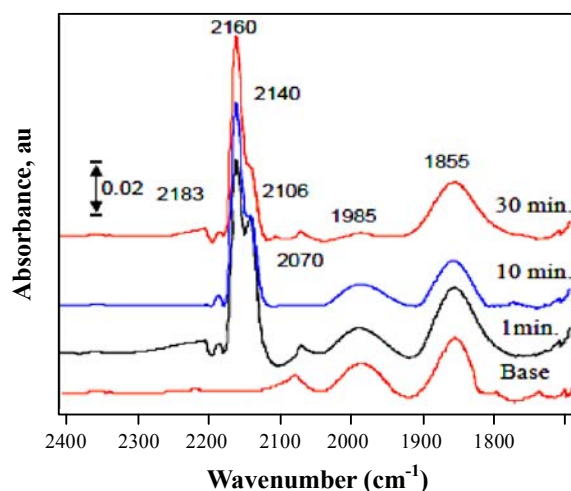


Fig. 9: *In situ* FTIR spectra of the CO + O₂ (10:10) gas mixture adsorbed on CuY as a function of contact time

CO oxidation over PtCuY

The promotion effect of Cu oxide on the activity of PtY towards CO oxidation in the presence of O₂ was studied by addition of CO + O₂ gas mixture and the spectra differences with changing contact time (1, 10, 50 and 70 min) are presented in Fig. 10. All the spectra showed the presence of a strong peak at 2154 cm⁻¹ due to Cu⁺-CO. Other two weak peaks at 2178 and 2065 cm⁻¹ were observed and they are attributed to Cu⁺(CO)₂ and M⁰-CO (M = Cu and/or Pt), respectively. Small peak at 1865 cm⁻¹ was observed as well which is due to bridged Pt⁰₂CO⁵⁵. Inspection of the spectra in Fig. 10a revealed that new peaks at 2353 and 1800-1600 cm⁻¹ were detected as well. These peaks are attributed to oxidation products of CO, which are CO₂ and carbonate/carboxylate, respectively^{56,57} on the surface of PtCuY catalyst. Increasing contact time as presented in Fig. 10b-d, leads to an increase in the intensity of the peak attributed to CO₂, however, the peaks in the range of 1800-1600 cm⁻¹ were maintained unchanged.

To declare the impact of reduction of PtCuY catalyst on CO oxidation, the gas mixture CO + O₂ was added to PtCuY(R) and the spectrum is shown in Fig. 10e. After admission, the gas was left until contact time of 70 min to compare with the spectrum of gas admission over unreduced PtCuY. Although, the spectrum showed that both samples presented the same group of peaks, the amount of physically adsorbed CO₂ (2353 cm⁻¹) that

is formed in case of the reduced sample was greatly higher than that in case of unreduced sample. This enhances the suggestion that, carbonate and carboxylate species are considered as intermediates of CO_2 formation.

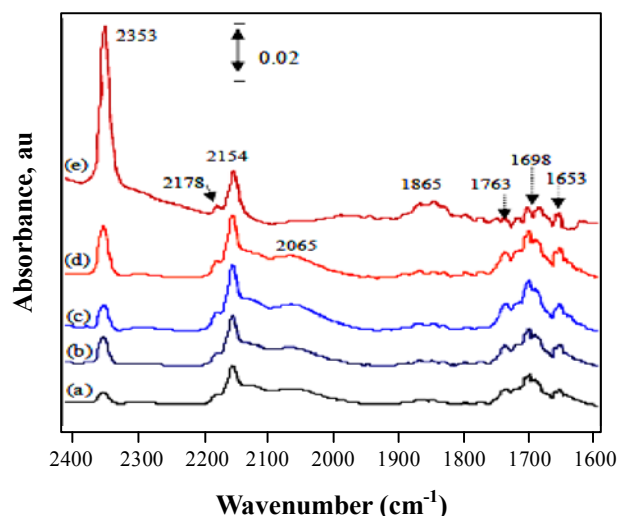


Fig. 10: *In situ* FTIR spectra of the $\text{CO} + \text{O}_2$ (10:10) gas mixture adsorbed on PtCuY for (a) 1 min, (b) 10 min (c) 50 min, (d) 70 min; and PtCuY(R) for (e) 70 min.

Water gas shift reaction

Water gas shift reaction over PtY

The IR spectra of PtY catalyst after admission of $\text{CO} + \text{H}_2\text{O}$ (15:1) as a function of the cell temperature are shown in Fig. 11. The initial spectrum after 0.5 min of contact time (Fig. 11a) shows small peaks at 2166 and 2074 cm^{-1} due to CO adsorbed on Pt cationic species ($\text{Pt}^{\text{n}+}\text{CO}$) and $\text{Pt}^0\text{-CO}$, respectively. Another peak at 1636 cm^{-1} was also observed. This peak may be attributed to carbonate species ($-\text{CO}_3^{2-}$) or $\delta(\text{H}_2\text{O})$ mode of adsorbed water, which lies in this region as well⁵⁸. It would be important to know the reason of this peak and whether it is due to carbonate species or $\delta(\text{H}_2\text{O})$. D_2O was used instead of H_2O and the same above procedure was applied. It was noticed that, this peak was not shifted upon using D_2O (not shown) confirming that this peak does not contain any hydrogen atom and hence it is assigned to carbonate species. This indicates the possibility of initiation of water gas shift reaction at room temperature at the surface of the employed catalyst. Increasing contact time to 20 min and then increasing the cell temperature to 50 and 100°C, Fig. 11b-d, leads to the increase of the peaks characteristic of carbonate species at 1636 cm^{-1} and the linear $\text{Pt}^0\text{-CO}$ at 2074 cm^{-1} which may be due to further reduction of $\text{Pt}^{\text{n}+}$ under the reaction conditions⁸.

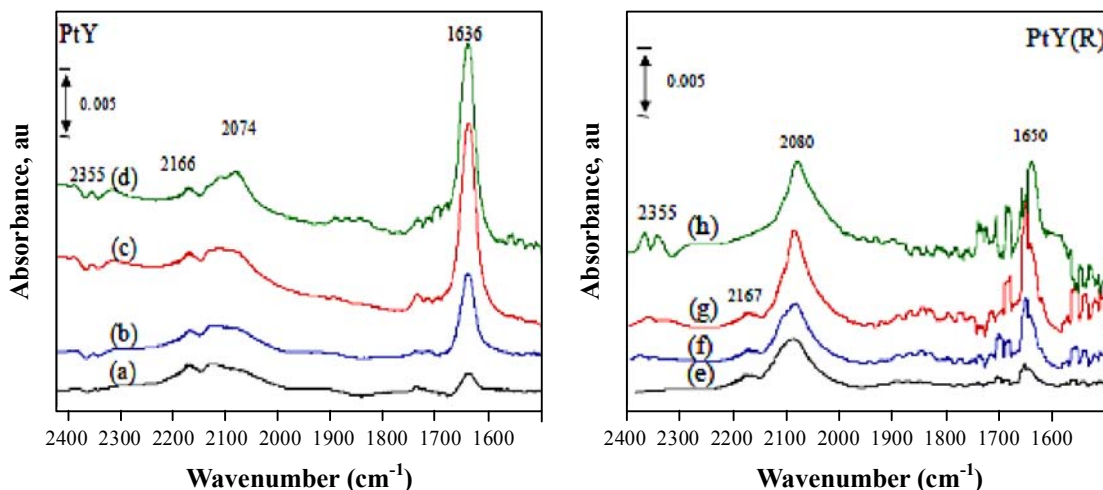


Fig. 11: *In situ* FTIR spectra of the CO + H₂O (15:1) gas mixture adsorbed on PtY and PtY(R) as a function of reaction time and temperature; (a and e) 0.5 min of gas adsorption at RT, (b and f) 20 min of gas adsorption at RT, (c and g) heated at 50°C and (d and h) heated at 100°C.

Adsorption of CO + H₂O (15:1) to PtY(R) leads to changes in the IR spectra as shown in Fig. 11. After 0.5 min of gas admission, the IR spectrum (Fig. 11e) showed peaks at 2167 and 2080 cm⁻¹ due to Ptⁿ⁺CO and Pt⁰-CO, respectively. The spectrum shows also small peak at 1650 cm⁻¹ related to carbonate species, which is considered as an oxidation product of CO in presence of H₂O. Fig. 11f-h presented the change of the spectra after increasing contact time to 20 min and increasing the cell temperature to 50 and 100°C. The spectra showed a slight increase of the peak at 1650 cm⁻¹ which is characteristic of carbonate species. Also, small peak at 2355 cm⁻¹ was also observed after heating the cell at 100°C. It is clear that, the intensity of carbonate species over unreduced PtY is greater than that over reduced PtY catalyst. Obviously, the yield of CO₂ is very small due to the shortage of O₂ in the cell atmosphere. It will be important to use O₂ in presence of H₂O as will be discussed later on.

Water gas shift reaction over PtCuY

Exposing PtCuY catalyst to the gas mixture of CO + H₂O (15:1) at RT and slightly change the cell temperature leads to some differences in the obtained spectra as presented in Fig. 12. The initial spectrum was recorded at room temperature and it did not show a significant effect in the transformation of CO in presence of H₂O (WGS). It presented only small peak at 1635 cm⁻¹, which is due to carbonate species (-CO₃²⁻). Increasing the cell temperature led to an increase in the peak at 1635cm⁻¹. Also a new peak was detected at

2353 cm^{-1} which is due to physically adsorbed CO_2 . Increasing the peak at 1635 cm^{-1} with increasing temperature confirms its relation with carbonate species at least after elevation of cell temperature. With more inspection of the recorded spectra, the peaks at 2180, 2153 and 2080 cm^{-1} increased. They are related to $\text{Cu}^+(\text{CO})_2$, Cu^+CO and $\text{M}^0\text{-CO}$ ($\text{M}=\text{Cu}$ and/or Pt), respectively. Finally, small peak at 1857 cm^{-1} , which is due to $\text{Pt}^0\text{-(CO)}_2$ was observed. With careful examination of Fig. 12, it can be observed that CO_2 increases on the expense of carbonate species. This may give an idea that, carbonate species is an intermediate to CO_2 on the surface of PtCuY. This conclusion is in agreement with that of the same reaction over PtY but it is different from PtFeY, however, CO_2 was reported as an intermediate of CO_3^{2-} ⁸.

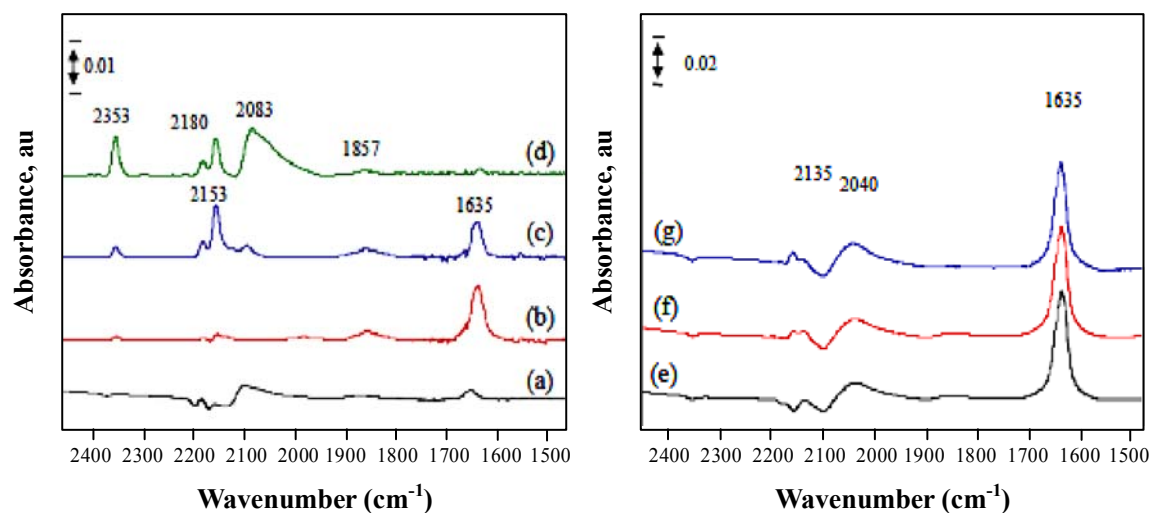


Fig. 12: *In situ* FTIR spectra of the $\text{CO} + \text{H}_2\text{O}$ (15:1) gas mixture adsorbed on PtCuY and PtCuY(R) as a function of reaction time and temperature; (a and e) one min of gas adsorption at RT, (b and f) 20 min of gas adsorption at RT, (c and g) heated at 50°C and (d) heated at 100°C

On the other hand, the spectra changes after admission of the gas mixture ($\text{CO} + \text{H}_2\text{O}$) to PtCuY(R) were presented in Fig. 12. It is clear that, the only CO oxidation product was carbonate species (1635 cm^{-1}) which started directly at RT. However, WGS reaction started after elevation of the cell temperature on the surface of unreduced catalyst, however, it did not change with elevation of the temperature. It is clear that, the amount of carbonate species (at 1635 cm^{-1}) on the surface of the reduced sample is greater than that on the surface of the unreduced sample which may be due to the shortage of O_2 . The formation of CO_2 (2353 cm^{-1}) on the expense of CO_3^{2-} (1635 cm^{-1}) strengthen the suggestion that, CO_3^{2-} is the intermediate of CO_2 on the surface of PtCuY catalyst.

Effect of water vapor on the oxidation of CO

A mixture of CO + O₂ containing trace amount of water vapor (CO:O₂:H₂O; 10:10:1) was admitted at RT to PtY and PtCuY catalysts in the IR cell. The spectra recorded after exposing PtY catalyst at RT (Fig. 13a) showed small peaks at 2082 and 1854 cm⁻¹ due to Pt⁰-CO and Pt⁰₂CO, respectively. Other small peaks at 2355 and 1641 cm⁻¹ due to CO₂ and carbonate species were also observed as CO oxidation products. Elevation of the cell temperature to 50 and 100°C (Fig. 13b,c) led to increase the intensity of CO₂ and carbonate species. The increase of the peaks intensity at 2355 and 1641 cm⁻¹ (CO oxidation products) may be due to the decrease of the CO adsorption strength which leads to CO desorption. Consequently, it leaves vacant sites for O₂ and H₂O and facilitates oxidation process since CO oxidation is accomplished according to Langmuir–Hinshelwood mechanism.

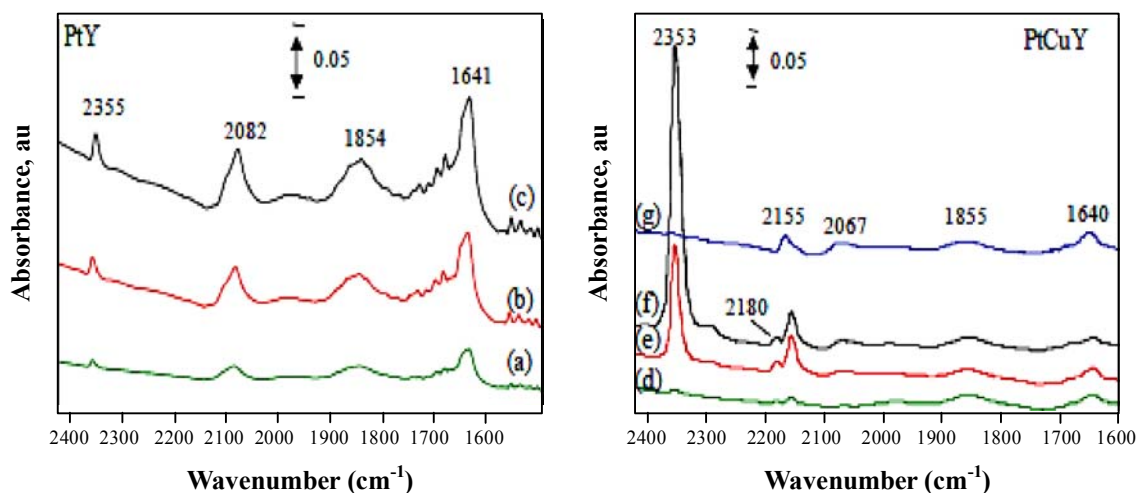


Fig. 13: *In situ* FTIR spectra of CO + O₂ + H₂O (15:15:1) adsorbed over PtY and PtCuY: (a and d) after 20 min at RT; (b and e) after heating at 50°C; (c and f) after heating at 100°C and (g) after evacuation at room temperature

The changes in the FTIR spectra after admission of the gas mixture (CO:O₂:H₂O; 10:10:1) to PtCuY in the range of 2400-1600 cm⁻¹ are shown in Fig. 13. The spectrum recorded at RT (Fig. 13d) did not show significant peaks except that small peak at 1640 cm⁻¹ due to carbonate species. Increasing the cell temperature to 100°C led to creation of small peaks at 2180, 2155, 2067 and 1855 cm⁻¹. These peaks are attributed to Cu⁺(CO)₂, Cu⁺-CO, M⁰-CO (M = Cu and/or Pt) and Pt₂CO, respectively. Also, it is clear that the CO₂ peak (2355 cm⁻¹) strongly increases with increasing temperature. From the change of this peak, it can be said that, the majority of CO was converted to CO₂, which is the same product after admission of CO + O₂ mixture. From these data, it is clear that, H₂O did not change the

reaction mechanism, however, it increases the conversion of CO to CO₂ on the surface of PtCuY catalyst because it is noticed that the major product was $-\text{CO}_3^{2-}$ in case of PtY, however, it was CO₂ in case of PtCuY. Since CO oxidation is accomplished according to Langmuir–Hinshelwood mechanism, the decrease of CO adsorption strength as discussed in TPD data leaves vacant sites for O₂ and H₂O. Therefore, the formation of CO₂ increases as oxidation product of CO in presence of O₂ and H₂O.

CONCLUSION

On the basis of physicochemical characterizations, it is concluded that addition of copper and/or platinum to Y zeolite did not change the its crystalline features. Addition of Cu to PtY reduced the platinum particle size from 20 to 14 nm in PtY and PtCuY, respectively. The CO and CO₂ desorption from bimetallic PtCuY was easier than that from single PtY catalyst. No peaks due to methanation were observed under the conditions of the present study. CO is mainly transforms to CO₂ in presence of O₂ while it transforms to carbonate in presence of H₂O. Water vapor enhances the oxidation of CO to CO₂ in presence of gas mixture of CO + O₂ + H₂O. According to the obtained data, carbonate species are considered as the intermediate of carbon dioxide on the surface of the prepared catalysts in this study.

REFERENCES

1. J. Yang, V. Tschamber, D. Habermacher, F. Garin and P. Gilot, *Appl. Catal. B*, **83**, 229-239 (2008).
2. U. R. Pillai and S. Deevi, *Appl. Catal. B*, **64**, 146-151 (2006).
3. A. K. Neyestanaki, F. Klingstedt, T. Salmi and D.Y. Murzin, *Fuel*, **83**, 395-408 (2004).
4. G. P. Chiusoli, P. M. Maitlis, *Platinum Metals Rev.* **51**, 187-188 (2007).
5. N. M. Marković and P. N. Ross Jr., *Surf. Sci. Rep.*, **45**, 117-229 (2002).
6. K. Arnby, M. Rahmani, M. Sanati, N. Cruise, A. Amberntsson and M. Skoglundh, *Appl. Catal. B*, **54**, 1-7 (2004).
7. M. Kotobuki, A. Watanabe, H. Uchida, H. Yamashita and M. Watanabe, *J. Catal.*, **236**, 262-269 (2005).
8. Z. M. El-Bahy, A. I. Hanafy, M. M. Ibrahim and M. Anpo, *J. Mol. Catal. A*, **344**, 111-121 (2011).

9. A. Sirijaruphan, J. G. Goodwin Jr. and R. W. Rice, *J. Catal.*, **224**, 304-313 (2004).
10. I. Tachard, A. C. B. da Silva, F. Argolo, S. M.O. Brito, H. O. Pastore, H. M. C. Andrade and A. J. S. Mascarenhas, *Stud. Surf. Sci. Catal.*, **167**, 195-200 (2007).
11. K. C. Khulbe, R. S. Mann and A. Manoogian, *Zeolites*, **7**, 228-230 (1987).
12. E. Smolentseva, N. Bogdanchikova, A. Simakov, A. Pestryakov, I. Tusovskaya, M. Avalos, M. H. Farías, J. A. Díaz and V. Gurin, *Surf. Sci.*, **600**, 4256-4259 (2006).
13. Z. M. El-Bahy, *Mater. Res. Bull.*, **42**, 2170-2183 (2007).
14. S. V. Didziulis, K. D. Butcher, S. L. Cohen and E. I. Solomon, *J. Am. Chem. Soc.*, **111**, 7110-7123 (1989).
15. E. I. Solomon, P. M. Jones and J. A. May, *Chem. Rev.*, **93**, 2623-2644 (1993).
16. T. S. Mozer and F. B. Passos, *Int. J. Hydrogen Energy*, **36**, 13369-13378 (2011).
17. L. E. Gómez, B. M. Sollier, M. D. Mizrahi, J. M. R. López, E. E. Miró and A. V. Boix, *Int. J. Hydrogen Energy*, **39**, 3719-3729 (2014).
18. J. Kugai, T. Moriya, S. Seino, T. Nakagawa, Y. Ohkubo, H. Nitani and T. A. Yamamoto, *Int. J. Hydrogen Energy*, **38**, 4456-4465 (2013).
19. P. Klug, L. E. Alexander, *Direction Procedures for Polycrystalline and Amorphous Materials*, Wiley (1954).
20. A. Parinyaswan, S. Pongstabodee and A. Luengnaruemitchai, *Int. J. Hydrogen Energy*, **31**, 1942-1949 (2006).
21. B. Atalik and D. Uner, *J. Catal.*, **241**, 268-275 (2006).
22. W. H. Quayle and J. H. Lunsford, *Inorg. Chem.*, **21**, 2226-2231 (1982).
23. A. Sirijaruphan, J. G. Goodwin and R. W. Rice Jr., *J. Catal.*, **221**, 288-293 (2004).
24. S. K. Jain, E. M. Crabb, L. E. Smart, D. Thompsett and A. M. Steele, *Appl. Catal. B*, **89**, 349-355 (2009).
25. M. H. Jordão, V. Simões and D. Cardoso, *Appl. Catal. A*, **319**, 1-6 (2007).
26. Z. M. El-Bahy, *Appl. Catal. A*, **468**, 175-183 (2013).
27. J. Scherzer and J. L. Bass, *J. Catal.*, **28**, 101-115 (1973).
28. R. Cid, F. J. Gil Lambfas, J. L. G. Fierro, A. Lopez Agudo and J. Villasenor, *J. Catal.*, **89**, 478-488 (1984).
29. S. Guerrero, J. T. Miller, A. J. Kropf and E. E. Wolf, *J. Catal.*, **262**, 102-110 (2009).

30. Y. Zang and R. Farnood, *Appl. Catal. B: Environ.*, **79**, 334-340 (2008).
31. P. Thormählen, M. Skoglundh, E. Fridell and B. Andersson, *J. Catal.*, **188**, 300-310 (1999).
32. R. Padilla, M. Benito, L. Rodríguez, A.S. Lotina and L. Daza, *J. Power Sources*, **192**, 114-119 (2009).
33. S.T. Hong, M. Matsuoka and M. Anpo, *Catal. Lett.*, **107**, 173-176 (2006).
34. S.H. Cho, J.S. Park, S.H. Choi and S.H. Kim, *J. Power Sources*, **156**, 260-266 (2006).
35. M. Kruk and M. Jaroniec, *Chem. Mater.*, **13**, 3169–3183 (2001).
36. K. Chakarova, M. Mihaylov and K. Hadjiivanov, *Micro. Meso. Mater.*, **81**, 305-312 (2005).
37. K. Chakarova, M. Mihaylov and K. Hadjiivanov, *Catal. Comm.*, **6**, 466-471 (2005).
38. K. Chakarova, K. Hadjiivanov, G. Atanasova and K. Tenchev, *J. Mol. Catal. A*, **264**, 270-279 (2007).
39. S. Albertazzi, G. Busca, E. Finocchio, R. Glöckler and A. Vaccari, *J. Catal.*, **223**, 372-381 (2004).
40. X. Liu, O. Korotkikh and R. Farrauto, *Appl. Catal. A*, **226**, 293-303 (2002).
41. M. Kantcheva, K. Hadjiivanov, A. Budneva and A. Davydov, *Appl. Surf. Sci.*, **55**, 49-55 (1992).
42. B. Busca, *J. Mol. Catal.*, **43**, 225-236 (1987).
43. A. Davydov, *IR Spectroscopy Applied to Surface Chemistry of Oxides*, Nauka, Novosibirsk (1984).
44. K. Hadjiivanov, M. Kantcheva and D. Klissurski, *J. Chem. Soc. Faraday Trans.*, **92**, 4595-4600 (1996).
45. Y. Itho, S. Nishiyama, S. Tsuruya and M. J. Masai, *J. Phys. Chem.*, **98**, 960-967 (1994).
46. G. J. Millar, C. H. Rochester and K. C. Waugh, *J. Chem. Soc. Faraday Trans.*, **88**, 1477-1488 (1992).
47. N.-Y. Topsoe and H. Topsoer, *J. Mol. Catal. A*, **141**, 95–105 (1999).
48. D. Scarano, S. Bordiga, C. Lamberti, G. Spoto, G. Ricchiardi, A. Zecchina and C. Otero Arean, *Surf. Sci.*, **411**, 272-285 (1998).
49. K. Hadjiivanov and L. Dimitrov, *Microp. Mesop. Mater.*, **27**, 49-56 (1999).

50. K. Hadjiivanov and H. Knözinger, *J. Catal.*, **191**, 480-485 (2000).
51. W. J. Bijsterbosh, F. Kapteigin and A. Moulijn, *J. Mol. Catal.*, **74**, 193-205 (1992).
52. G. Ghiotti, F. Bocuzzi and A. Chiorino, *Stud. Surf. Sci. Catal.*, **21**, 235-246 (1985).
53. G. Ertl, *Surf. Sci.*, **299**, 742-754 (1994).
54. J. Winterlin, S. Völkening, T. V. W. Janssens, T. Zambelli and G. Ertl, *Science*, **278**, 1931-1934 (1997).
55. E. Ivanova, M. Mihaylov, F. Thibault-Starzyk, M. Daturi and K. Hadjiivano, *J. Mol. Catal. A*, **274**, 179-184 (2007).
56. Z. M. El-Bahy, *Mod. Res. Catal.*, **2**, 136-147 (2013).
57. I. Tankov, W. H. Cassinelli, J. M. C. Bueno, K. Arishtirova and S. Damyanova, *Appl. Surf. Sci.*, **259**, 831-839 (2012).
58. M. Ahrens, O. Marie, P. Bazin and M. Daturi, *J. Catal.*, **271**, 1-11 (2010).

Revised : 18.03.2016

Accepted : 20.03.2016